LASER INTERFEROMETER GRAVITATIONAL WAVE OBSERVATORY
- LIGO -
CALIFORNIA INSTITUTE OF TECHNOLOGY
MASSACHUSETTS INSTITUTE OF TECHNOLOGY

Technical Note **LIGO-T1300633–v1** 2013/08/08

Quantum-noise reduction schemes for future advanced gravitational-wave detectors Progress report 2

Mikhail Korobko, Haixing Miao, and Yanbei Chen

California Institute of Technology
LIGO Project, MS 18-34
Pasadena, CA 91125
Phone (626) 395-2129
Fax (626) 304-9834
E-mail: info@ligo.caltech.edu

Massachusetts Institute of Technology
LIGO Project, Room NW22-295
Cambridge, MA 02139
Phone (617) 253-4824
Fax (617) 253-7014
E-mail: info@ligo.mit.edu

LIGO Hanford Observatory
Route 10, Mile Marker 2
Richland, WA 99352
Phone (509) 372-8106
Fax (509) 372-8137
E-mail: info@ligo.caltech.edu

LIGO Livingston Observatory
19100 LIGO Lane
Livingston, LA 70754
Phone (225) 686-3100
Fax (225) 686-7189
E-mail: info@ligo.caltech.edu

http://www.ligo.caltech.edu/

1 Quantum noises

Contemporary so-called second-generation gravitational-wave detectors, such as Advanced LIGO [1, 2], Advanced VIRGO [3], and KARGA [4], which are under construction now, will be quantum noise limited over the detection frequency band. At low frequencies, it is dominated by the radiation pressure noise which is due to quantum fluctuation in the amplitude of the optical field [5]; while at high frequencies, the shot noise dominates which arises from the phase fluctuation. There is a trade-off between these two noises that is called Standard Quantum Limit (SQL) [6]. In the linear position meter (the gravitational-wave interferometer is special case of it) the shot noise corresponds to the measurement noise and radiation pressure noise to the back-action noise. The SQL is not an ultimate limit for measurement precision: there are several methods of overcoming it in gravitational-wave detectors. The most well-known examples are Quantum Non-Demolition (QND) measurements and Back-Action Evading (BAE) measurements (see, *e.g.*, [7, 8, 9, 10]). The first method tries to measure conserved dynamical quantity of the system [6, 7, 11, 12]. The second method uses the correlation between the measurement noise and the back-action noise [10, 13, 14, 15, 16, 17].

Though there are many various approaches, applicable for different special cases (*e.g.*, for the certain frequency range), the community looks for other solutions. In this work we investigate multiple optical springs approach.

2 Optical rigidity

The Hamiltonian of a system with a resonator (length L and resonant frequency ω_c) with one movable mirror (resonant frequency ω_0) which motion is being measured by laser (with frequency ω_0):

$$\hat{\mathcal{H}} = \frac{\hbar\omega_m^2}{2}\hat{x}^2 + \frac{\hat{p}^2}{2m} + \hbar\omega_c\hat{e}^\dagger\hat{e} + \hbar G_0\hat{x}\hat{e}^\dagger\hat{e} + i\hbar\sqrt{2\gamma}\left(\hat{a}\hat{e}^\dagger e^{-i\omega_0 t} - \hat{a}^\dagger\hat{e}e^{-i\omega_0 t}\right) \tag{1}$$

The first term corresponds to the mechanical mode ($[\hat{x},\hat{p}] = i\hbar$). The second one describes the cavity mode with annihilation operator $\hat{e}$ and commutator $[\hat{e},\hat{e}^\dagger] = 1$. The third is interaction between the oscillator and light with optomechanical coupling constant $G_0 = \omega_0/L$. The last term describes the pump $\hat{a}$, where γ is half-bandwidth of the resonator.

This Hamiltonian can be linearized if we assume the pump is big so we can replace the operators by the sum of the mean value and small perturbation:

$$\hat{e} \to \bar{e} + \hat{e}, \qquad \hat{e} \ll \bar{e}.$$

Then in the rotating wave approximation we get linearized Hamiltonian:

$$\hat{\mathcal{H}} = \frac{\hbar\omega_m^2}{2}\hat{x}^2 + \frac{\hat{p}^2}{2m} + \hbar\delta\hat{e}^\dagger\hat{e} + \hbar G_0\hat{x}(\hat{e}^\dagger\bar{e} + \bar{e}^*\hat{e}) + i\hbar\sqrt{2\gamma}\left(\hat{a}\hat{e}^\dagger - \hat{a}^\dagger\hat{e}\right) \tag{2}$$

where $\delta = \omega_c - \omega_0$ is detuning. We can assume that $\bar{e}$ is real value, so we can simplify the equation by the substitution $g = G_0\bar{e}$.

The Hamilton equation is [18]:

$$\dot{\hat{e}} = -\frac{i}{\hbar}[\hat{e}, \hat{\mathcal{H}}] - \gamma a \tag{3}$$

We find:

$$\dot{\hat{e}} + (\gamma + i\delta)\hat{e} = -ig\hat{x} + \sqrt{2\gamma}\hat{a} \tag{4}$$

For the output signal we have [18]:

$$\hat{b} = -\hat{a} + \sqrt{2\gamma}\hat{e} \tag{5}$$

The same we can derive for the mechanical mode, and get the system of Langevin equations:

$$\begin{cases} \dot{\hat{e}} + (\gamma + i\delta)\hat{e} = -ig\hat{x} + \sqrt{2\gamma}\hat{a} \\ \dot{\hat{x}} = \frac{\hat{p}}{m} \\ \dot{\hat{p}} + \gamma_m\hat{p} = -m\omega_m^2\hat{x} + \hbar g(\hat{e}^\dagger + \hat{e}) + \hat{\zeta}_{th} \end{cases} \tag{6}$$

where $\hat{\zeta}_{th}$ is Brownian thermal force with correlation function

$$\langle\hat{\zeta}_{th}(t)\hat{\zeta}_{th}(t')\rangle = 2m\gamma_m k_B T\delta(t - t').$$

For the cavity mode in the spectral representation we can get:

$$\hat{e}(\omega) = \frac{g\hat{x}(\omega) + i\sqrt{2\gamma}\hat{a}(\omega)}{\omega - \delta + i\gamma} \tag{7}$$

$$\hat{e}^\dagger(\omega) = \frac{-g\hat{x}(\omega) + i\sqrt{2\gamma}\hat{a}(-\omega)}{\omega + \delta + i\gamma} \tag{8}$$

For the mechanical mode from (6) we get:

$$m(\ddot{\hat{x}} + \gamma_m\dot{\hat{x}} + \omega_m^2\hat{x}) = -\hbar g(\hat{e}^\dagger + \hat{e}) + \hat{\zeta}_{th} = F_{BA} + \hat{\zeta}_{th} \tag{9}$$

Calculate the back-action term:

$$F_{BA} = \hbar g(\hat{e}^\dagger + \hat{e}) = -\hbar g\left\{g\hat{x}(\omega)\left(\frac{1}{\omega - \delta + i\gamma} - \frac{1}{\omega + \delta + i\gamma}\right) + i\sqrt{2\gamma}\left(\frac{\hat{a}^\dagger}{\omega + \delta + i\gamma} + \frac{\hat{a}}{\omega - \delta + i\gamma}\right)\right\} =$$
$$= -\frac{2\hbar g^2\delta\hat{x}(\omega)}{(\omega - \delta + i\gamma)(\omega + \delta + i\gamma)} + 2\hbar g\sqrt{\gamma}\frac{\hat{a}_1(\gamma - i\omega) + \delta\hat{a}_2}{(\omega - \delta + i\gamma)(\omega + \delta + i\gamma)} = -\mathcal{K}(\omega)\hat{x}(\omega) + \hat{F}_n(\omega) \tag{10}$$

where

$$\hat{a}_1 = \frac{\hat{a} + \hat{a}^\dagger}{\sqrt{2}}, \hat{a}_2 = \frac{\hat{a} - \hat{a}^\dagger}{i\sqrt{2}},$$

and we also introduce optical rigidity $\mathcal{K}$ and noise term $\hat{F}_n$.

The dynamics of the system can be described by:

$$\hat{x}(\omega) = \chi_{eff}(\omega)[\hat{F}_n + \hat{\zeta_{th}} + G], \tag{11}$$

where G is signal and

$$\chi_{eff}^{-1}(\omega) = -m\omega^2 + \mathcal{K}(\omega) \tag{12}$$

So the optical rigidity effectively modifies the dynamics of the mirror.

3 Spectral density

Now let's descibe the output in simplier way. From the equations Eq.(7),(5) we can derive the two-photon ouput quadratures:

$$\hat{\mathbf{b}}(\omega) = \mathbb{R}\hat{a}(\omega) + 2\sqrt{\gamma}\mathbb{L}\hat{X}(\omega) \tag{13}$$

where

$$\mathbb{L} = \frac{1}{\mathcal{D}(\omega)}\begin{bmatrix}\gamma - i\omega & -\delta \\ \delta & \gamma - i\omega\end{bmatrix} \tag{14}$$

$$\mathcal{D}(\omega) = (\gamma - i\omega)^2 + \delta^2 \tag{15}$$

$$\hat{X}(\omega) = \bar{E}\frac{k_0\hat{x}(\omega)}{\sqrt{\tau}}\begin{bmatrix}0\\1\end{bmatrix}, \qquad k_0 = \omega_0/c, \qquad \tau = L/c \tag{16}$$

$$\mathbb{R} = 2\gamma\mathbb{L} - \mathbb{I} \tag{17}$$

and $\bar{E}$ is amplitude of the classical field in the cavity. In the single-mode approximation the field in the cavity is:

$$\hat{\mathbf{e}}(\omega) = \frac{\mathbb{L}(\omega)}{\sqrt{\tau}}\left(\sqrt{\gamma}\hat{a} + \hat{X}(\omega)\right) \tag{18}$$

Thus the back-action force is:

$$F_{BA} = \frac{2\hbar k_0\bar{E}}{\sqrt{\tau}}\hat{\mathbf{e}}(\omega)\begin{bmatrix}1\\0\end{bmatrix}^T = F_n - \mathcal{K}(\omega)\hat{x}(\omega) \tag{19}$$

where

$$F_n = \frac{2\hbar k_0\bar{E}\sqrt{\gamma}}{\sqrt{\tau}}\mathbb{L}(\omega)\begin{bmatrix}1\\0\end{bmatrix}^T \tag{20}$$

$$\mathcal{K}(\omega) = \frac{mJ\delta}{\mathcal{D}(\omega)}, \qquad J = \frac{4\omega_0 I_c}{mcL} = \frac{4\hbar k_0^2\bar{E}^2}{m\tau} \tag{21}$$

which is exactly what we get in the equation (10) As we mentioned before the optical spring term $\mathcal{K}$ can be included in mechanical susceptibility term, thus the dynamics of the system is:

$$\hat{x}(\omega) = \chi_{xx}^{eff}(\omega)\left[\hat{F}_n + G(\omega)\right] \tag{22}$$

where G is external classical force and effective susceptibility is:

$$\chi_{xx}^{eff\,-1} = \chi_{xx}^{-1} + \mathcal{K}(\omega) = -m(\omega^2 + i\gamma_m\omega - \omega_m^2) + \mathcal{K}(\omega) \tag{23}$$

In general the system can be described by the system:

$$\begin{cases}\hat{\mathcal{O}}(\omega) = \hat{\mathcal{O}}^{(0)}(\omega) + \chi_{OF}(\omega)\hat{x}(\omega) \\ \hat{F}(\omega) = \hat{F}^{(0)}(\omega) + \chi_{FF}\hat{x}(\omega) \\ \hat{x}(\omega) = \chi_{xx}^{eff}(\hat{F}_n(\omega) + G(\omega))\end{cases} \tag{24}$$

where $\hat{\mathcal{O}}$ is output from the measurement system and $\hat{F}$ is the back-action force. The measurement result we get by applying measurement operator $\mathbf{H}$ to the output $\hat{b}$. In the case of homodyne detection:

$$\hat{\mathcal{O}}(\omega) = \mathbf{H}^{\mathrm{T}}\hat{\mathbf{b}}(\omega) = \begin{bmatrix}\cos\zeta \\ \sin\zeta\end{bmatrix}^{\mathrm{T}} \begin{bmatrix}\hat{b}_c \\ \hat{b}_s\end{bmatrix} = \hat{b}_c\cos\zeta + \hat{b}_s\sin\zeta \tag{25}$$

In our case these parameters are:

$$\chi_{OF}(\omega) = 2\frac{k_0\sqrt{\gamma}}{\sqrt{\tau}}\mathbf{H}^{\mathrm{T}}\mathbb{L}(\omega)\bar{E}\begin{bmatrix}0\\1\end{bmatrix} \tag{26}$$

$$\hat{\mathcal{O}}^{(0)} = \mathbf{H}^{\mathrm{T}}\mathbb{R}\hat{a} \tag{27}$$

$$\chi_{FF}(\omega) = -\mathcal{K}(\omega) \tag{28}$$

$$\hat{F}^{(0)} = \frac{2\hbar k_0\bar{E}\sqrt{\gamma}}{\sqrt{\tau}}\begin{bmatrix}1\\0\end{bmatrix}^{T}\mathbb{L}(\omega)\hat{a} \tag{29}$$

The system (24) can be resolved:

$$\hat{\mathcal{O}}(\omega) = \hat{\mathcal{O}}^{(0)}(\omega) + \frac{\chi_{xx}^{eff}\chi_{OF}}{1-\chi_{xx}^{eff}\chi_{FF}}\left[G(\omega)+\hat{F}^{(0)}\right] \tag{30}$$

This can be renormalized to the more convenient form. In particular, we can consider the signal as sum of the classical force and some noise:

$$\hat{\mathcal{O}}^{F}(\omega) = \hat{\mathcal{N}}^{F} + G(\omega) = \frac{\hat{\mathcal{X}}}{\chi_{xx}^{eff}(\omega)} + \hat{\mathcal{F}}(\omega) + G(\omega) \tag{31}$$

where

$$\hat{\mathcal{X}}(\omega) = \frac{\hat{\mathcal{O}}^{(0)}(\omega)}{\chi_{OF}(\omega)} = \sqrt{\frac{\hbar}{\gamma m J}}\frac{\mathcal{D}(\omega)}{\mathbf{H}^{\mathrm{T}}\mathbf{D}}\mathbf{H}^{\mathrm{T}}\mathbb{R}\hat{a} \tag{32}$$

$$\mathbf{D}(\omega) = \mathcal{D}(\omega)\mathbb{L}(\omega)\begin{bmatrix}0\\1\end{bmatrix} = \begin{bmatrix}-\delta\\ \gamma - i\omega\end{bmatrix} \tag{33}$$

$$\hat{\mathcal{F}}(\omega) = \hat{F}_n = \sqrt{mJ\hbar\gamma}\begin{bmatrix}1\\0\end{bmatrix}^{\mathrm{T}}\mathbb{L}(\omega)\hat{a} \tag{34}$$

The spectral density of output can be calculated:

$$S^{F}(\omega) = \frac{S_{\mathcal{X}\mathcal{X}}}{|\chi_{xx}^{eff}|^2} + S_{\mathcal{F}\mathcal{F}} + 2\Re\left\{\frac{S_{\mathcal{X}\mathcal{F}}}{\chi_{xx}^{eff}}\right\} \tag{35}$$

And the corresponding spectral densities are:

$$S_{\mathcal{X}\mathcal{X}} = \frac{\hbar}{4\gamma m J}\frac{|\mathcal{D}(\omega)^2|}{\mathbf{H}^{\mathrm{T}}\mathbf{D}\mathbf{D}^{\dagger}\mathbf{H}}\mathbf{H}^{\mathrm{T}}\mathbb{R}\mathbb{R}^{\dagger}\mathbf{H} = \frac{\hbar}{4\gamma m J}\frac{1}{\left|\mathbf{H}^{\mathrm{T}}\mathbb{L}\begin{bmatrix}1\\0\end{bmatrix}\right|^2} \tag{36}$$

$$S_{\mathcal{F}\mathcal{F}} = \gamma m\hbar J\begin{bmatrix}1\\0\end{bmatrix}^{\mathrm{T}}\mathbb{L}\mathbb{L}^{\dagger}\begin{bmatrix}1\\0\end{bmatrix} \tag{37}$$

$$S_{\mathcal{X}\mathcal{F}} = \frac{\hbar}{2}\frac{\mathcal{D}(\omega)}{\mathbf{H}^{\mathrm{T}}\mathbf{D}}\mathbf{H}^{\mathrm{T}}\mathbb{R}\mathbb{L}^{\dagger}\begin{bmatrix}1\\0\end{bmatrix} = \frac{\hbar}{2}\frac{\mathbf{H}^{\mathrm{T}}\mathbb{L}\begin{bmatrix}1\\0\end{bmatrix}}{\mathbf{H}^{\mathrm{T}}\mathbb{L}\begin{bmatrix}0\\1\end{bmatrix}} \tag{38}$$

It's useful to have these spectral densities in different normalizations. The connection between them is:

$$S^x = S^F|\chi_{xx}^{eff}|^2 \tag{39}$$

$$S^h = S^F\left(\frac{2}{mL\omega^2}\right)^2 \tag{40}$$

4 Multiple Optical Springs

In this approach, we are not trying to use some precise techniques of the noise cancellation (like in back-action evasion), but modifying the dynamics of test mass and therefore enhance the response of the detector to the gravitational-wave signal (amplify this signal). In other words, the fact that the SQL for the force depends on the dynamics of the mirrors allows us to modify this dynamics in the way to overcome the free-mass SQL.

The equation of motion for the position of the test mass x describes the dynamics of the system:

$$x(\Omega) = \chi(\Omega)F(\Omega), \tag{41}$$

where $\chi(\Omega)$ is a mechanical susceptibility and $F(\Omega)$ is an external force. In case of free mass the susceptibility is simply $-1/m\Omega^2$, but in the case of detuned Fabry-Pérot cavity with one movable mirror we have to add another term (optical rigidity $K(\Omega)$) to the susceptibility which describes the interaction:

$$\chi(\Omega) = \big(-m\Omega^2 + K(\Omega)\big)^{-1}. \tag{42}$$

This term is similar to the one describing the spring in the oscillator, that is why this phenomenon is called optical spring [19, 20, 21]. The idea, proposed in the paper [22], is to use the frequency dependence of the optical rigidity to compensate the inertia term, and therefor to decrease the force SQL, that depends on the susceptibility [23]:

$$S_F^{SQL}(\Omega) = 2\hbar|\chi^{-1}(\Omega)|, \tag{43}$$

and thus the larger we can make the susceptibility the better precision we get.

4.1 Two optical springs

While the frequency and cavity bandwidth is much smaller than detuning, we can expand the optical rigidity in Taylor series:

$$K \approx \bar{K} - i\Gamma_{opt}\Omega - m_{opt}\Omega^2 + \mathcal{O}(\Omega^3), \tag{44}$$

where

$$\bar{K} = \frac{mJ\delta}{(\delta^2+\gamma^2)^2}, \qquad \Gamma_{opt} = -\frac{2mJ\gamma\delta}{(\gamma^2+\delta^2)^4}, \qquad m_{opt} = -\frac{MJ\delta(\delta^2-3\gamma^2)}{(\delta^2+\gamma^2)^2} \tag{45}$$

As soon as $\bar{K}, \Gamma_{opt}, m_{opt}$ depend only on the parameters of the system: cavity bandwidth, cavity detuning and renormalized optical power, we can choose the m_{opt} in the way to compensate the positive inertia and thus if we combine two carriers we can cancel the constant $\bar{K}_{1,2}$ and inertia terms:

$$\bar{K}_1 + \bar{K}_2 = 0, \qquad m + m_{opt,1} + m_{opt,2} = 0. \tag{46}$$

This canceling significantly reduce the force SQL comparing to the free mass one (in Eq. (42) and (43) we do not take into account the damping term proportional to Ω):

$$\frac{[S_F^{SQL}]_{\text{modified}}}{[S_F^{SQL}]_{\text{free mass}}} = \left|\frac{[\chi(\Omega)_{\text{modified}}]}{m\Omega^2}\right| \approx \left|\frac{|m_{opt}| - m}{m}\right|. \tag{47}$$

By changing the effective mass $|m_{opt}| \to m$ we can achieve the ratio much smaller than one.

This approach works at low frequencies and breaks down at high frequencies since we have to take into account higher terms of Taylor series (44) and that limits us in achieving better sensitivity in broader frequency range.

4.2 Multiple optical springs

The idea that follows directly from this feature - add more optical springs and thus cancel the higher terms of the Taylor expansion. Unfortunately that doesn't work well, because the parameter space becomes very large and it's impossible to solve the equations.

Thus the other approach is to minimize the response in some frequency band. That means we have to minimize functional $G[\chi_{eff}^{-1}]$ that depends on the effective susceptibility with N optical springs:

$$\chi_{eff}^{-1}(\omega) = -m\omega^2 + \sum_{i=0}^{N} \mathcal{K}_i(\omega) \tag{48}$$

Each $\mathcal{K}_i$ has three parameters to optimize: J_i, δ_i, γ_i, thus the parameter space has $3N$ dimensions.

We can think about two possible goals of the optimization:

- Make the response function constant over some frequency band. Then the SQL (43) will be constant and we'll be able to achieve it in any point.
- Make the effective mass smaller and remove higher order frequency dependence. That means, that response curve that we want to get is parallel to the $m\omega_0^2$ curve.

5 Optimization of the response function

5.1 Cost function

The most naive functional that directly maximizes the response is:

$$G_1 = \int_{f_{min}}^{f_{max}} \ln |\chi_{eff}^{-1}(f)|^2 \, d \ln f \tag{49}$$

It doesn't specify the shape of the final curve, so, in order to achieve goals we stated before, we can create the functional, that will give us either constant susceptibility or with very small effective mass:

$$G_2 = \int_{f_{min}}^{f_{max}} \ln |\chi_{eff}^{-1}(f) - \text{const}|^2 \, d \ln f, \tag{50}$$

$$G_3 = \int_{f_{min}}^{f_{max}} \ln |\chi_{eff}^{-1}(f) - \Delta m (2\pi f)^2|^2 \, d \ln f, \tag{51}$$

The other approach is to minimize the maximum of the function over the frequency band. In this case functionals are:

$$G_4 = \max_f \ln |\chi_{eff}^{-1}(f) - \text{const}|^2 \tag{52}$$

$$G_5 = \max_f \ln |\chi_{eff}^{-1}(f) - \Delta m (2\pi f)^2|^2 \tag{53}$$

$$\tag{54}$$

where *const* is some constant, Δm is smaller than m. Finally, the absolute can be expanded into squares of real and imaginary part of susceptibility and we can add weight to each of them - then we get so-call multi-objective optimization:

$$G_6 = \max_f \ln \left(a \Re \left[\chi_{eff}^{-1}(f) \right]^2 + b \Im \left[\chi_{eff}^{-1}(f) \right]^2 \right) \tag{55}$$

where a, b - weights. The algorithm we used here is particle swarm optimization (see Appx.A). Maximization of the function in $G_{4,5,6}$ was done by Sequential Least Squares Programming (SLSQP) [24]. Result of the optimization is on Fig. 1. Similar plots we get for any figure of merit G_i. The explanation of it is simple - there's a point, where $\chi_{eff}^{-1}(f) = 0$, thus optimization can't avoid falling in this pit.

The other approach is to make Taylor expansion up to high-order terms and then minimize coefficients of this expansion with different weights:

$$G_7 = a \left(\sum_i K_i(0) \right)^2 + b \left(i \sum_i K_i'(0) \right)^2 + c \left(\frac{1}{2} \sum_i K_i''(0) - m \right)^2 + d \left(\frac{i}{6} \sum_i K_i'''(0) \right)^2 + \ldots \tag{56}$$

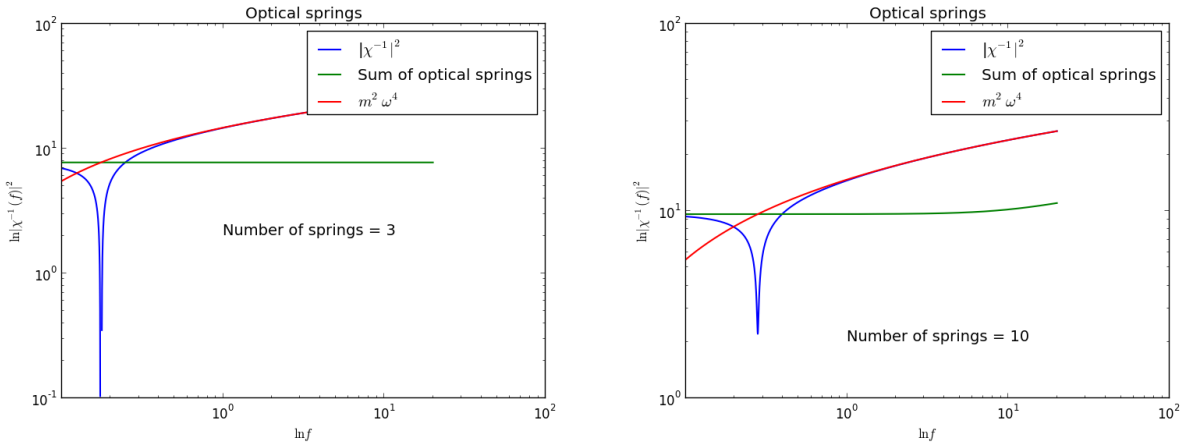

Figure 1: Effective susceptibility comparing to the free mass one.

Unfortunately this approach gives us the same result as previous ones.

The next step is creating more complex functional, that takes into account both first derivative (it should change gradually and with proper rate to help us avoid the dips) and second derivative (this is optional, but rather useful).

The other option is to use properties of the function's shape - we discuss that in the next section.

5.2 Vector fitting

As we show above, the usual minimization doesn't work as wanted, so we propose using another method, called vector fitting [25, 26]. Its idea is quite simple - we fit into data the function of form:

$$f(s) = \sum_{i=1}^{N} \frac{c_i}{s - a_i} + d + sh \tag{57}$$

where $s = i\omega$, c_i are residuals, a_i are poles and d, h are some constants. In general c_i, a_i can be pares of complex conjugated values. This method works in two steps: on the first step it determines poles of the function and on the second step it uses least squares method to fit linear functino of residuals to the data. More details about the algorithm can be found in the original paper [25].

In our case we can rewrite the optical spring term:

$$\mathcal{K}(s) = \frac{mJ\delta}{(\gamma - s)^2 + \delta^2} = \frac{mJ\delta}{(\gamma + i\delta - s)(\gamma - i\delta - s)} = \frac{m}{2}\left(\frac{-iJ}{s - (\gamma + i\delta)} + \frac{iJ}{s - (\gamma - i\delta)}\right) \tag{58}$$

So for the algorithm we should put

$$a_i = \gamma - i\delta, \qquad a_{i+1} = a_i^*, \qquad c_i = iJ, \qquad c_{i+1} = c_i^* = -iJ, \qquad h = 0. \tag{59}$$

Then the idea is to fit this kind of function into $m\omega^2$ and thus achieve only constant $1/d$ total response function.

6 Discussion and future plans

The system that we investigate has many parameters to change and optimize, so it should be very flexible for achieving the goal, but the figure of merit for such optimization is not obvious. The research that we have done in Section 5.1 shows that direct optimization can't provide us the result we want to get — broad-band reduction of reverse effective susceptibility. Nevertheless, we have two options for the further work: creating function of merit with derivatives and vector fitting algorithm. The last one looks more promising, so it is the next step of the work. After (and if) we find a way to reduce the susceptibility we should think about construction of the output spectral density. It should be some optimal combination of output channels, as described in [27]. Moreover, each output has it's own homodyne detection angle, and whole system should be optimized over all the angles in order to achieve the best sensitivity.

References

[1] www.advancedligo.mit.edu.

[2] G.M.Harry (for the LIGO Scientic Collaboration), Classical and Quantum Gravity **27**, 084006 (2010).

[3] http://wwwcascina.virgo.infn.it/advirgo/.

[4] http://gwcenter.icrr.u-tokyo.ac.jp/en/.

[5] C. Caves, Physical Review D (1981).

[6] V.B.Braginsky, F.Ya.Khalili, *Quantum Measurement*, Cambridge University Press, 1992.

[7] V. B. Braginsky, F. Ya. Khalili, Physics Letters A **147**, 251 (1990).

[8] A. Buonanno and Y. Chen, Physical Review D **64**, 1 (2001).

[9] F.Ya.Khalili, Physics Letters A **288**, 251 (2001).

[10] H.J.Kimble, Yu.Levin, A.B.Matsko, K.S.Thorne and S.P.Vyatchanin, Physical Review D **65**, 22002 (2001).

[11] V.B.Braginsky, Yu.I.Vorontsov, F.Ya.Khalili, Sov.\,Phys.\,JETP **46**, 705 (1977).

[12] V. B. Braginsky, F. Ya. Khalili, Review of Modern Physics **68**, 1 (1996).

[13] W.G.Unruh, in *Quantum Optics, Experimental Gravitation, and Measurement Theory*, edited by P.Meystre and M.O.Scully, page 647, Plenum Press, New York, 1982.

[14] F.Ya.Khalili, Doklady Akademii Nauk **294**, 602 (1987).

[15] M.T.Jaekel and S.Reynaud, Europhysics Letters **13**, 301 (1990).

[16] A.F.Pace, M.J.Collett and D.F.Walls, Physical Review A **47**, 3173 (1993).

[17] S.P.Vyatchanin and A.B.Matsko, Sov. Phys. JETP **83**, 690 (1996).

[18] D. Walls and G. Milburn, Quantum Optics, 2008.

[19] H.Rehbein, H.Mueller-Ebhardt, K.Somiya, S.L.Danilishin, R.Schnabel, K.Danzmann, Y.Chen, Physical Review D **78**, 062003 (2008).

[20] A. Buonanno and Y. Chen, Classical and Quantum Gravity , 8 (2002).

[21] A. Buonanno and Y. Chen, Physical Review D , 1 (2002).

[22] F. Khalili, S. Danilishin, and H. Müller-Ebhardt, Physical Review D **1**, 1 (2011).

[23] S. L. Danilishin, Living Rev. Relativity (2012).

[24] P. Boggs and J. Tolle, Acta numerica (1995).

[25] B. Gustavsen and A. Semlyen, Power Delivery, IEEE Transactions ... **14**, 1052 (1999).

[26] B. r. Gustavsen, Power Delivery, IEEE Transactions on **21**, 1587 (2006).

[27] H. Rehbein, M. Helge, K. Somiya, and L. Stefan, page 1.

[28] Y. Shi and R. Eberhart, ... The 1998 IEEE International Conference on (1998).

[29] J. Kennedy, Encyclopedia of Machine Learning (2010).

[30] R. Poli, Journal of Artificial Evolution and Applications (2008).

[31] R. Eberhart and Y. Shi, ..., 2000. Proceedings of the 2000 Congress ... (2000).

[32] R. Mendes, (2004).

[33] G. Evers and M. B. Ghalia, Systems, Man and Cybernetics, 2009. ..., 3901 (2009).

[34] P. Yin, F. Glover, M. Laguna, and J. Zhu, ... Journal of Swarm Intelligence ... (2011).

[35] X. Xie, W. Zhang, and Z. Yang, ... 2002. CEC'02. Proceedings of the ... **2**, 1456 (2002).

A Particle Swarm Optimization

The particle swarm optimization (PSO)[28, 29] is genetic algorithm that doesn't require gradient of the function and good initial guess for the parameters. It works good with multi-dimensional problems, where usual methods cannot give good convergence. It is used widely [30] in all kinds of optimization problems.

General idea is the following: algorithm has several candidate solutions (called particles) and moves them iteratively, changing the position and velocity of each particle in parameter space using simple rule, that brings the swarm of particles in the minimum after some time. The algorithm is the following:

- Initialize particles randomly from the parameter space and set these coordinates as best known position of i-th particle p_i
- Evaluate the fitness of the initial population
- Choose the best fitness $f(g)$ between them, and the coordinates of the best particle is g
- While termination criteria is met:
  - For each particle:
    - Update the velocity of the particle:

$$v_i \leftarrow \chi(v_i + \varphi_1 U(0,1)(p_i - x_i) + \varphi_2 U(0,1)(g - x_i))$$

    - Update the position of the particle: $x_i \leftarrow x_i + v_i$
    - If the fitness $f(x_i) < f(p_i)$:
      - Update best known position of the particle: $p_i = x_i$
      - If the fitness $f(x_i) < f(g)$: update best known global position $g = x_i$

Here $U(0,1)$ is random number from region $(0,1)$ and we choose parameters of the scheme to provide convergence [31]:

$$\chi = \frac{2}{|2 - (\varphi_1 + \varphi_2) - \sqrt{(\varphi_1 + \varphi_2)^2 - 4(\varphi_1 + \varphi_2)}}, \qquad \varphi_1 = 2.05, \qquad \varphi_2 = 2.05$$

Unfortunately PSO algorithm tends to get in local minimums, and in order to avoid this property some modifications were proposed [32, 33, 34] and we chose dissipative PSO [35], which randomly resets speed or velocity of the particle, adding the dissipation to the system.